Tetrahedron 75 (2019) 2118–2127

Contents lists available at ScienceDirect

Tetrahedron

journal homepage: www.elsevier.com/locate/tet

Revisiting the reduction of indoles by hydroboranes: A combined experimental and computational study

Arumugam Jayaraman [a], Henry Powell-Davies [b], Frédéric-Georges Fontaine [a, *, 1]

[a] Département de Chimie, Université Laval, 1045 Avenue de la Médecine, Québec City, Québec G1V 0A6, Canada
[b] School of Chemistry, Cardiff University, Cardiff, Cymru/Wales, UK

ARTICLE INFO

Article history:
Received 14 December 2018
Received in revised form
14 February 2019
Accepted 22 February 2019
Available online 27 February 2019

Keywords:
Indoles
Hydroboration
Frustrated Lewis pairs
Hydroboranes
Homogeneous catalysis
Metal-free catalysis

ABSTRACT

A combined experimental and density functional computational study was used to probe the mechanism for the reduction of indoles using simple borane BH_3·DMS (DMS = dimethyl sulfide). Experimental and computational studies all steer to the formation of the reduced species 1-BH_2-indolines as the resting state for this reaction, as opposed to the historically presumed formation of the unreduced 1-BH_2-indoles, before the addition of a proton source to form the final product indolines. Furthermore, it was observed that molecular H_2 was generated and consumed in the reaction. Computations put forward hydroboration followed by protodeborylation as the very reasonable mechanistic route for the formation of experimentally observed major intermediate 1-BH_2 indolines. For the H_2 consumption in the reaction, computations suggest the frustrated Lewis pair-type heterolytic splitting of H_2 by a bis(3-indolinyl) borane intermediate.

1. Introduction

The reduction of *N*-H indoles to indolines has been an ubiquitous reaction within the organic chemistry community and can be done using either transition metal catalysis [1] or simple stoichiometric reduction using hydroboranes [2]. For the latter, borohydrides such as $NaBH_4$, $NaBH_3(CN)$ or boranes, mostly on the form BH_3·Lewis base, were employed along with a proton source. Reduction of indoles using borohydrides in the presence of a proton source was commonly presumed to proceed via an indolenium ion, by protonation of an indole substrate, followed by the addition of a hydride, leading to the desired indoline (Scheme 1a) [2a-c]. The same reaction using boranes, either B_2H_6 or BH_3·base, was postulated to proceed via the 1-BH_2-indole intermediate, formed through dehydrogenative coupling of an initial B-N complex (BH_3-indole) (Scheme 1b) [2g]. This intermediate subsequently abstracts a proton and a hydride in sequence to form the final indoline. While the latter mechanism for the reduction of indoles using boranes seems reasonable, indoles were generally regarded to exhibit enamine reactivity from the heterocyclic chemistry perspective [3].

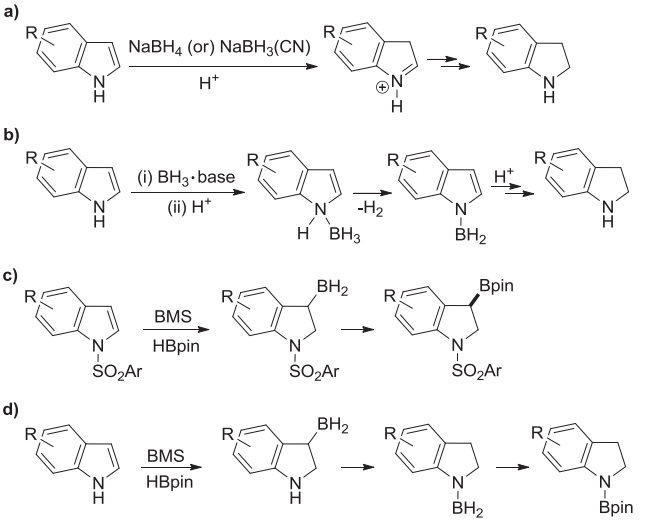

Scheme 1. Previously established mechanistic pathways (a–c) for reaction of protected and unprotected indoles with hydroboranes, and this current work (d) of a proposed reaction pathway for the reduction of indoles using hydroboranes. BMS = trihydridoborane dimethylsulfide complex.

* Corresponding author.
E-mail address: frederic.fontaine@chm.ulaval.ca (F.-G. Fontaine).
[1] Canada Research Chair in Green Catalysis and Metal-Free Processes.

https://doi.org/10.1016/j.tet.2019.02.048
0040-4020/

Hydroboration of enamines using boranes, leading to vicinal aminoboranes, at ambient and low temperature is well documented [4]. Our recent exploration of the reactivity of ambiphilic aminoboranes and simple hydroboranes toward N-protected indoles [5] revealed that hydroboration of indoles takes place when an electron withdrawing group (EWG) is present at the N-position, leading to formation of air and moisture-sensitive 3-boryl indoline intermediates (Scheme 1c). These unstable intermediates were trapped using HBpin, which led to stable 3-Bpin indolines. Recent studies on the reactivity of boranes without any hydride substituent toward *N*-protected indoles and enamines also showed compelling evidences for a strong interaction between boranes and the C3 of indoles and enamines [6]. With this fresh understanding on the reactivity of protected indoles with a variety of boranes and the availability of new trapping techniques and modern instrumentations, we report herein our exploration of the reactivity of unprotected indoles with catalytic and stoichiometric amount of simple hydroboranes (Scheme 1d), and the various mechanistic possibilities for this deep-rooted reduction reaction.

2. Results and discussion

2.1. Catalytic reactions

In analogy to our previous report on the BH_3-catalyzed borylative dearomatization of 1-arylsulfonyl indoles [7], we looked at the effect of a catalytic quantity of borane dimethyl sulfide complex (BMS, 5 mol%) in presence of the unprotected parent indole and 2 equiv of pinacolborane (HBpin). When the reaction was carried out under strict water-free conditions either at room temperature (RT) for 16 h or at 60 °C for 3 h, 1-Bpin indoline (**2a**) was observed along with ~1 equiv of unreacted HBpin (Scheme 2). This result is surprising since the expected 1,3-diboryl indoline, which should form by the tandem BH_3-catalyzed hydroboration of the alkene part of the pyrrole ring and dehydrogenative N–B coupling, was not observed.

The reduction of the aromatic C(2)-C(3) moiety to two chemically inequivalent methylene units in product **2a** was apparent from NMR spectroscopy, where the ^{1}H NMR spectrum showed two triplets at δ 3.06 and 3.78 and the ^{13}C(APT) spectrum unambiguously showed two negative phase signals at δ 29.6 and 47.1. ^{11}B NMR spectroscopy and mass spectrometry also confirm the identity of **2a**. Other unprotected indoles that bear synthetically useful functionalities on the benzene ring, as shown in Scheme 3, provided similar results. Substrates such as 7-fluoro indole (**1m**) and 7-methyl indole (**1n**), however, led only to a moderate conversion, and no catalytic reaction was observed with 2,3-dimethyl indole (**1o**) and 1,2,3,4-tetrahydrocarbazole (**1p**) [8]. While most of the 1-Bpin indoline products were formed quantitatively, their purification by means of crystallization or column chromatography was not possible because of their facile hydrolysis, leading to the formation of indoline derivatives. Formation of 1-Bpin indoline derivatives is also viable through dehydrogenative coupling between unprotected indolines and HBpin in the presence of catalytic amount of BMS [9]. Albeit, the use of indoles to form such products can be ideal in the perception of atom economy, as this synthetic route accumulates no by-product.

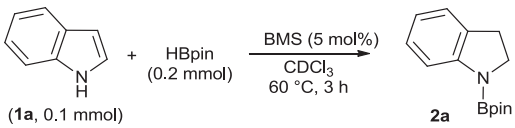

Scheme 2. Reduction of indole using HBpin in the presence of catalytic BMS. BMS = trihydridoborane dimethylsulfide complex.

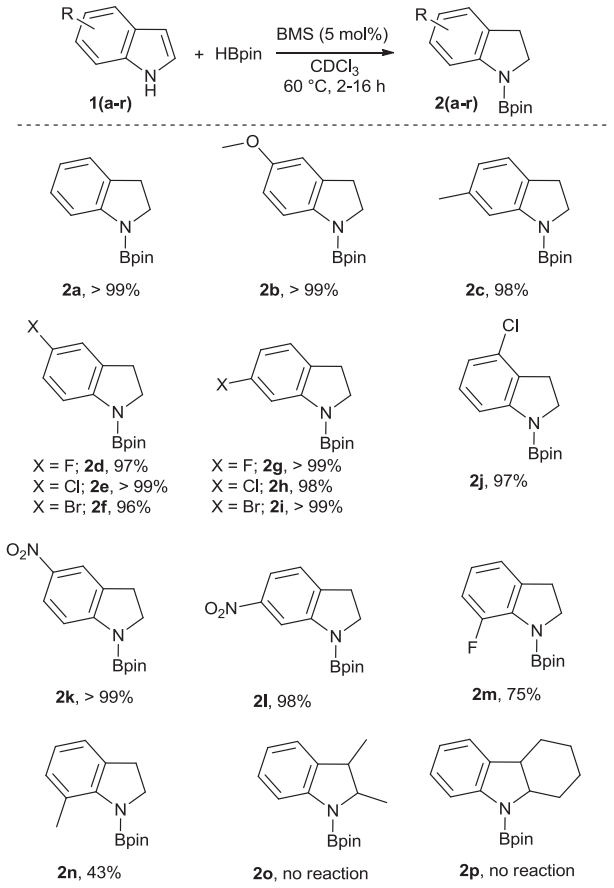

Scheme 3. Reduction of various indoles using HBpin and catalytic BMS, with conversions obtained from ^{1}H NMR (referenced from corresponding unreacted indole derivative) spectroscopy. BMS = trihydridoborane dimethylsulfide complex.

2.2. Stoichiometric reactions

To gain some mechanistic insight into how this catalytic reaction occurs, indole was treated with different molar ratios of BMS at different temperatures and reaction time in J. Young NMR tubes. The reaction conditions and results of these reactions are displayed in Table 1. With 1 equiv of BMS, the indole substrate disappeared completely after one hour at RT. Nevertheless, the reaction was incomplete as the ^{1}H and ^{11}B NMR spectroscopy reveal that a substantial amount of unreacted BMS was present in addition to the indoline-BH_3 complex (**3a**), molecular H_2, 1-BH_2 indoline (presumably in its dimeric form **4a**), and diindolinyl borane **5a** (entry 1).

Heating the same solution to 60 °C for 2 h resulted in a decrease of the proportion of BMS, complete disappearance of the indoline-BH_3 complex (**3a**) and molecular H_2, and appearance of species **4a** in major proportion and species **5a** in a significant proportion (entry 2) [10]. With 2 equivalents of BMS at 60 °C after 2 h, species **4a** was observed as the major species (entry 3). On the other hand, under the same reaction conditions but with 0.5 equivalent of BMS, the formation of species **5a** was observed in majority (entry 4). Since indoline-BH_3 complex (**3a**) is only observed at room temperature, it becomes obvious that it is an intermediate that transforms to the more stable 1-BH_2 indoline (**4a**). Furthermore, comparison of the last two reactions (entries 3 and 4) with entry 2 suggests that disproportionation can take place where species **4a** can form **5a** with a concomitant release of BMS. The extent of the

Table 1
Outcomes of the reaction of indole with few different equivalents of BMS at different temperature.

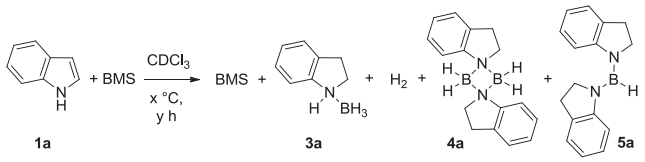

entry	1a:BMS	x (°C)	y (h)	BMS (%)[a]	3a (%)[a]	4a (%)[a]	5a (%)[a]
1[c]	1:1	RT	1	45	8.5	12[b]	28
2	1:1	60	2	25	0	44[b]	31
3	1:2	60	2	19	0	76[b]	5
4	1:0.5	60	2	0	0	6[b]	94

[a] The percentage is based on ^{11}B NMR integration.
[b] The percentage mentioned is for the amount of boron atoms and is based on monomeric species (**4a′**) instead of the dimeric species **4a**, which would be half.
[c] Based on the ^{1}H NMR integration, some amount of H_2 is present in solution.

disproportionation depends on the stoichiometry of BMS used in the reaction. This relation is important when looking at the catalytic transformations in Scheme 3 since a 20:1 ratio of indole to BMS should favor the presence of analogues of **5a** rather than species **4a**. In all cases, we did not observe any evidence of the presence of species 1-BH_2-indole, although we cannot definitely confirm that it cannot exist in undetectable concentrations.

Next, in an attempt to understand the generation of 1-Bpin indoline (**2a**), a stoichiometric amount of HBpin was added to the mixture of 1-BH_2 indoline (**4a**) and diaminoborane (**5a**) arising from the 1:1 reaction between indole and BMS. This reaction resulted in complete disappearance of the diaminoborane species **5a** and appearance of product **2a** at RT after 16 h (Scheme 4). Surprisingly, only a small portion of major species **4a** was consumed, even at elevated temperature (60 °C). Interestingly, it suggests that higher yields of **2** are expected under catalytic conditions where a deficiency of BMS will be present relative to the parent indoles.

2.3. Revisiting the mechanism of indole reduction using BH_3 solvates

Reduction of unprotected indoles to indolines using a stoichiometric amount of BH_3·THF and the mechanistic details of this reaction have been studied half a century ago by Schmidt et al. [2g] In their study, formation of the species 1-BH_2 indole was postulated as the resting state (Scheme 1b). Furthermore, it was reported that the establishment of this resting state accompanies a stoichiometric amount of H_2 liberation. Lastly, to obtain the final indoline product a prerequisite for a stoichiometric amount of a proton source, such as methanol, which involves in protonation of the 1-BH_2 indole intermediates, was mentioned. While their mechanistic proposal seems logical, our experimental observations as mentioned in the previous section for the reaction between indole and BMS evidently diverges from their mechanistic proposal. Some of our experimental inferences include formation of the reduced species 1-BH_2 indoline (**4a**) without addition of any external proton source and generation of minor amount of H_2 in the reaction.

Due to the disparity between the previous and current experimental outcomes from the reaction of indole with simple hydroboranes, a further mechanistic scrutiny for this reaction is warranted. For this purpose, DFT computations at the ωB97XD/6-31g(d,p) level of theory were performed and are discussed in the following sections.

2.4. Computed dehydrogenative coupling route vs hydroboration route

Computations were first aimed at comprehending if the dehydrogenative N-borylation of indoles occurs first, as proposed by Schmidt and coworkers [2g]. In line with their proposal, the formation of 1-boryl indole intermediate (**I2**) and H_2 from indole and BMS is thermodynamically favorable ($\Delta G = -14.6$ kcal/mol; Fig. 1, red and green lines). However, in contrast to their hypothesis, the formation of initial N-B complex (**I1**) from indole and BMS is less favored as this step is endergonic by 9.1 kcal/mol. Moreover, formation of the postulated species 1-BH_2 indole (**I2**) and H_2 from reactants via a direct dehydrogenative coupling transition state (**TS(1−2)**, green line), as proposed by Bertrand et al. for the dehydrocoupling of primary and secondary amines with HBpin [11], is kinetically inept as the $\Delta G^{\ddagger}$ is 30.7 kcal/mol. This barrier is too high to support the experimental reactivity at RT or 60 °C. Alternatively, the BH_3-assisted dehydrocoupling transition state (**TS(1−2)′**, red line), as evidenced previously by Shore et al. for the dehydrogenative coupling of amine-boranes [12], is kinetically favorable compared to the previous route, as the transition state holds a barrier of 26.3 kcal/mol. Nevertheless, both processes are significantly higher in energy compared to the hydroboration of indole, which has a transition state (TS) barrier of 19.6 kcal/mol. As expected, the *syn* addition of H and BH_2 groups at C2 and C3 position,

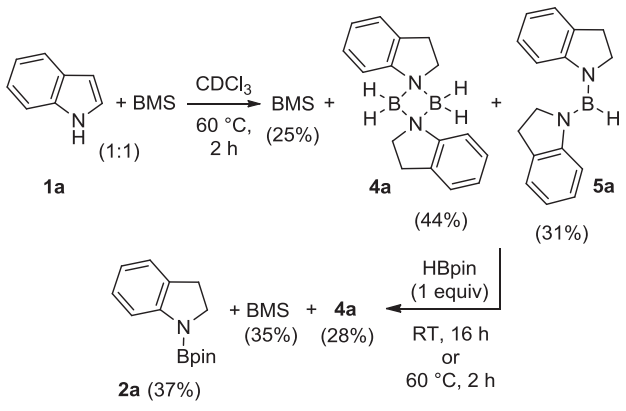

Scheme 4. Reaction sequence for the transformation of indole to 1-Bpin indoline using stoichiometric BMS and HBpin. BMS = trihydridoborane dimethylsulfide complex.

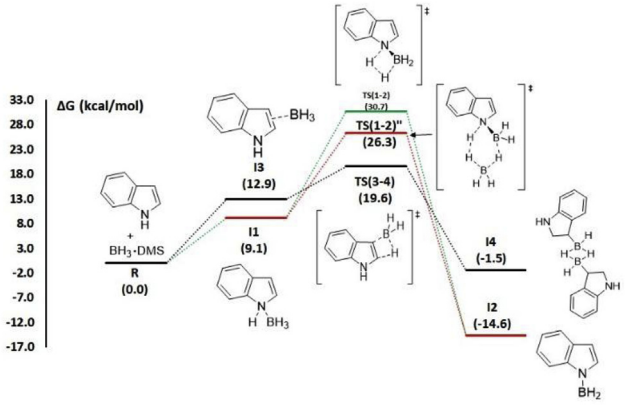

Fig. 1. Computed dehydrogenative coupling routes (green and red lines) for formation of 1-BH_2 indole, and the hydroboration route (black line) to furnish 3-BH_2 indoline intermediate.

respectively, is kinetically more favored over the addition of boron at the C2 position ($\Delta G^{\ddagger} = 23.0$ kcal/mol).

2.5. Pathways for the formation of 1-BH_2 indoline (**4a**) from 3-BH_2 indoline intermediate (**I4**)

As the hydroboration route seems favored, we explored next the possible pathways to generate 1-BH_2 indoline intermediate (**4a**) from the 3-BH_2 indoline intermediate (**I4**). For this purpose, it was first considered for species **I4** to undergo a bimolecular protodeborylation process, leading to formation of indoline and 1,3-di-BH_2 indoline (**A**; Scheme 5, first step). As we have initially observed the species indoline-BH_3 complex (**3a**) from the stoichiometric reaction conducted at RT (see Table 1, entry 1), we next supposed that Lewis basic indoline can coordinate with the unreacted BMS to form **3a**. From this species, two pathways were conceived for the formation of the observed 1-BH_2 indoline (**4a**). In the first pathway, species **3a** reverses back to give indoline, which in turn reacts with 1,3-di-BH_2 indoline (**A**) through a protodeborylation transition state to afford only species **4a** (Scheme 5, pathway a). In the second pathway, the indoline-BH_3 complex **3a** undergoes either direct or BH_3-assisted dehydrogenative coupling to furnish **2a** along with equimolar amount of H_2 (Scheme 5, pathway b).

From the analysis of the computed free energy profile for these two pathways (Fig. 2), the pathway a (black line) that involves protodeborylation is slightly favored over pathway b (red and green lines) that encompasses the dehydrogenative coupling processes. For pathway a, the protodeborylation step from indoline-BH_3 complex (**3a**) was rate limiting ($\Delta G^{\ddagger} = 23.1$ kcal/mol, step **I8** to **TS(9–10)**). For pathway b, the BH_3-assisted dehydrocoupling step from species **3a** was rate limiting ($\Delta G^{\ddagger} = 24.5$ kcal/mol, step **I8** to **TS(8–11)′**). Since the rate limiting barriers of both pathways are only 1.4 kcal/mol apart from each other, the BH_3-assisted dehydrocoupling route of pathway b should be considered as kinetically competitive to pathway a. This phenomenon clarifies how a minor amount of H_2 was generated from the reaction of indole with BMS. The facile hydroboration of indole by BMS, and the succeeding deborylation processes of the formed 3-BH_2 indoline intermediate to furnish the observed 1-BH_2 indoline species (**4a**) clearly demonstrates that no external proton source is needed for the reduction of indole. The N-H functionality of indoline or 3-BH_2 indoline serves as an internal proton source. Experiments carried out using 1-D indole also support this view, as the deuterium atom was transferred exclusively to the C3 of 1-BH_2 indoline product (see Fig. S7 in the Supplementary Material).

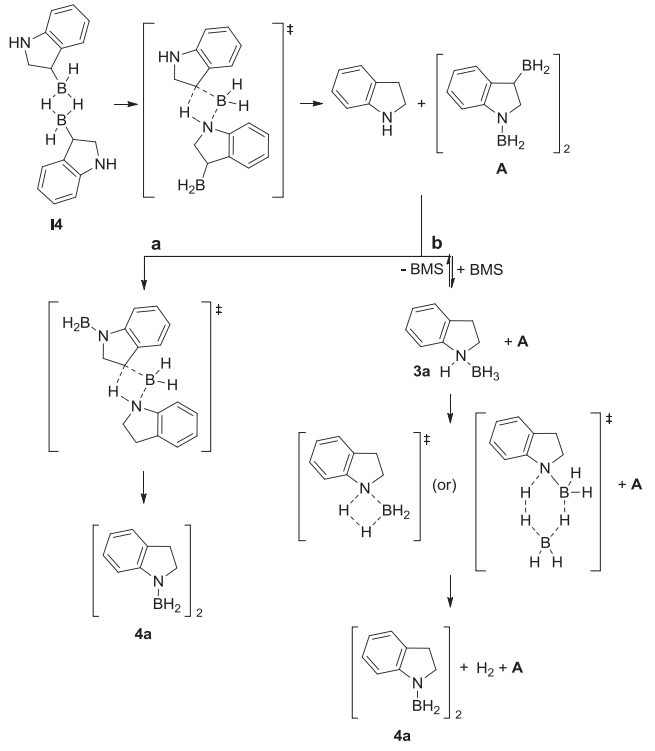

Scheme 5. Conceived pathways for the formation of 1-BH_2 indoline (**4a**) from 3-BH_2 indoline intermediate (**I4**). Pathway a involves protodeborylation, and pathway b entails BH_3 complexation followed by dehydrocoupling.

2.6. Pathways for formation of 1-BH_2 indoline (**4a**) via the 3H-indole-BH_3 complex (**6a**)

As another possible pathway for the formation of 1-BH_2 indoline (**4a**) from indole and BMS, a tautomeric switch of indole from its 1*H* form to 3*H* form, followed by coordination of it to BH_3 of BMS, and subsequent rearrangements to the desired **4a** was considered (Scheme 6). Indoles are generally known to exist in two tautomeric forms, 1*H* and 3*H* [13]. The equilibrium is dependent on the nature of the substituents on indoles and the pH of the solution. For example, 2-alkoxy indoles were reported to predominantly exist in their 3*H* tautomeric form [14]. The spontaneous 1*H*-to-3*H* tautomeric switch was also observed for certain indoles under aqueous conditions [15]. To ascertain the extent by which this tautomerism contributes to the formation of the observed species **4a** from the reaction between indole and BMS, the spontaneous equilibrium between the two tautomeric forms of selected indoles were computed. From the results listed in Table 2, only 2-methoxy indole was shown to spontaneously exist in its 3*H* form (entry 1). For other derivatives, the equilibrium lies far towards their 1*H* form, although with different endergonic energetics (entries 2–10). Therefore, presumably none of the indoles we examined experimentally may undergo a spontaneous switch to their 3*H* tautomer.

Whereas several 1*H*-indoles may not undergo spontaneous tautomerization, Resconi and coworkers have demonstrated that in the presence of a strong Lewis acidic borane, $B(C_6F_5)_3$, various indoles can be converted to 3*H*-indole-$B(C_6F_5)_3$ complexes [16]. The computed thermodynamics for the formation of the 3*H*-indole-$B(C_6F_5)_3$ complex from 1*H*-indole and $B(C_6F_5)_3$ shows that this step is exergonic by 10.3 kcal/mol. The analogous calculations using boranes, BMS and BH_3·THF, and 1*H*-indole disclosed that the formation of 3*H*-indole-BH_3 complex (**6a**) is exergonic as well ($\Delta G = -2.7$ and -3.7 kcal/mol, respectively). These results have driven us to continue exploring the mechanistic pathways for the rearrangement of species **6a** to 1-BH_2 indoline (**4a**).

The step going from **6a** to **4a** was exergonic with a ΔG of -25.3 kcal/mol (Fig. 3; step **I13** to **I14**). However, the barrier for this step through a direct 1,3-hydride shift from boron to C2 was found higher ($\Delta G^{\ddagger} = 28.5$ kcal/mol; red line). Interestingly, the BH_3-assisted transition state lowered the barrier down to 19.6 kcal/mol (black line). Despite the fact that the 1,3-hydride shift step from stage **I13** to **I14** to form the ultimate 1-BH_2 indoline (**4a**) seems feasible both thermodynamically and kinetically, the formation of the 3*H*-indole-BH_3 complex (**6a**) from 1*H*-indole and BMS appears to be less possible. This step through an initial B-N adduct (**I12**) formation followed by the DMS-assisted 1,3- proton shift from nitrogen to C3 appears kinetically inaccessible as it expresses a barrier of 34.8 kcal/mol (the first two mechanistic steps of Fig. 3). Hence, if an alternative lower energy pathway exists to reach 3*H*-indole-BH_3 complex (**6a**) from 1*H*-indole and BMS, then this whole mechanistic pathway should be considered as a competing route to

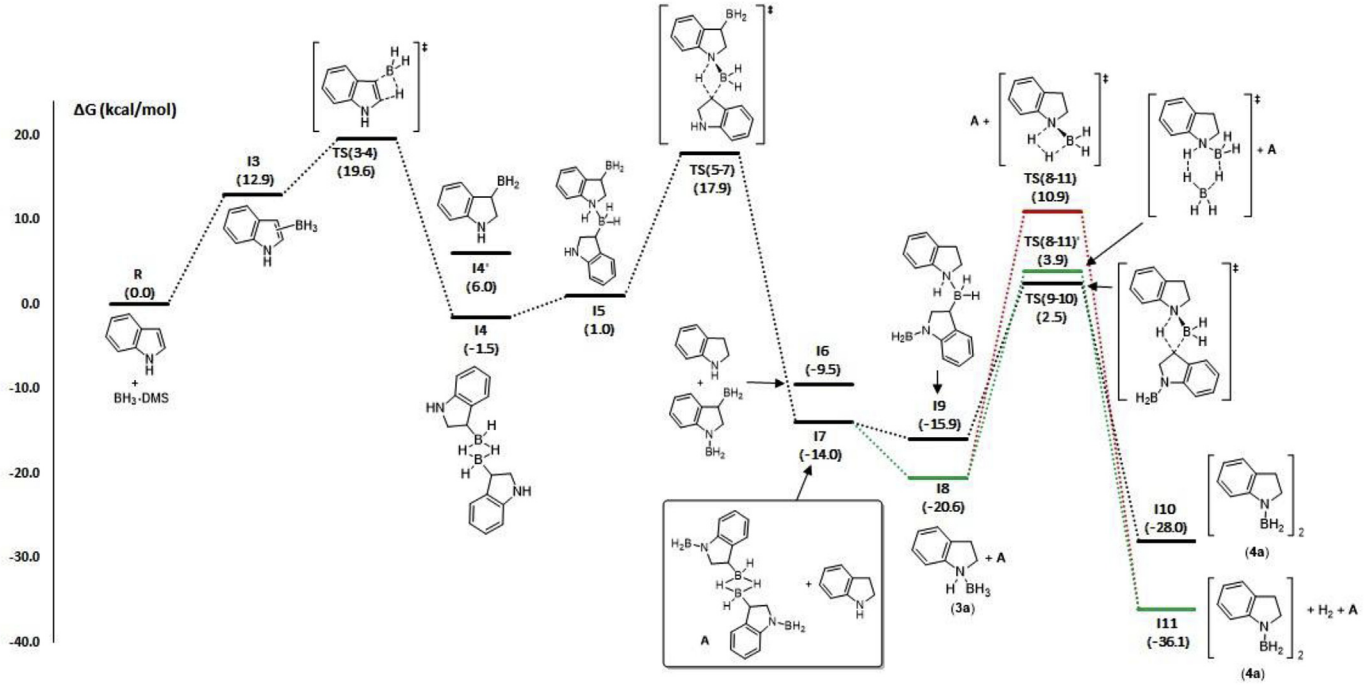

Fig. 2. Computed different mechanistic pathways for the formation of resting state **4a** using the hydroborated intermediate **I4**.

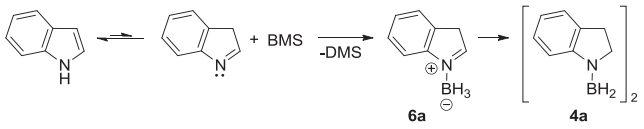

Scheme 6. A pathway conceived for the formation of 1-BH_2 indoline (**4a**) from indole and BMS via 3*H*-indole-BH_3 complex (**6a**).

Table 2
Computed free energy difference (in kcal/mol) between selected 1*H*-indoles and their 3H-indole tautomers.

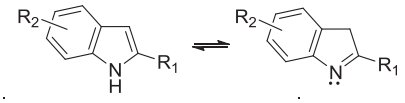

entry	substrate	ΔG (kcal/mol)
1	2-methoxy-1*H*-indole	−1.6
2	1*H*-indole	8.6
3	5-methoxy-1*H*-indole	6.1
4	5-fluoro-1*H*-indole	8.4
5	5-chloro-1*H*-indole	8.9
6	5-nitro-1*H*-indole	10.1
7	6-fluoro-1*H*-indole	8.7
8	6-chloro-1*H*-indole	9.1
9	6-nitro-1*H*-indole	10.7
10	4-chloro-1*H*-indole	8.6

the first proposed hydroboration/self protodeborylation route, but none was found in our hands.

2.7. Pathways for consumption of H_2

One important experimental feature of the stoichiometric transformation was the consumption of initially evolved minor dihydrogen towards generation of **4a** and **5a**. For the investigation

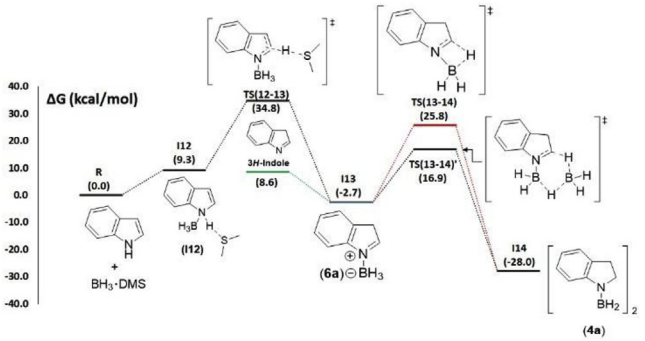

Fig. 3. Computed mechanistic pathways for rearrangement of 3*H*-indole-BH_3 complex (**6a**) to 1-BH_2 indoline (**4a**).

of mechanistic pathways for H_2 consumption, two pathways were considered (Scheme 7). In the first pathway (pathway a), the monomeric form (**I4′**) of 3-BH_2 indoline intermediate (**I4**) was viewed as an intramolecular vicinal frustrated Lewis pair (FLP), where the Lewis acid is the borane and the Lewis base is the nitrogen of indoline. Frustrated Lewis pairs [17], both intra- and intermolecular varieties, are widely known to activate the H-H bond of molecular hydrogen [18]. Repo demonstrated that a similar BH_2 containing aminoborane can reversibly activate dihydrogen [18e]. As a result, the species **I4′** was anticipated to cleave molecular H_2 and afford a zwitterion intermediate (**I16**), which may subsequently transform to the indoline-BH_3 complex (**3a**) through a self protodeborylation process. In the second pathway (pathway b), the 3-BH_2 indoline intermediate (**I4**) initially hydroborates another indole substrate and forms the secondary borane (**I18**). This thought came from the fact that several examples of dihydroboration by treating BH_3·base with over 2 equiv of alkenes, including cyclic olefins, and 1-arylsulfonyl indoles have been previously reported [19]. In the next step of pathway b, the secondary borane **I18** cleaves H_2 in a similar fashion as that of **I4′** and forms the zwitterion **I19**, which may further transform to the indoline-3-

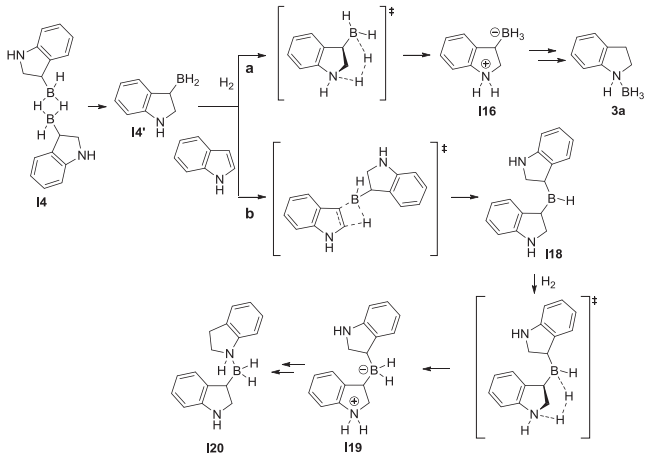

Scheme 7. Pathways for the consumption of generated H_2 in the reduction reaction. Pathway a involves H_2 cleavage by 3-BH_2 indoline (**I4′**), and pathway b involves H_2 cleavage by the dialkylborane **I20**.

BH_2 indoline complex (**I20**) by a self protodeborylation process. For pathway a, the computed structure of the monomeric 3-BH_2 indoline intermediate (**I4′**) is displayed in Fig. 4a. The structure of this species indeed exhibits an important property of intramolecular frustrated Lewis pairs, which is the right orientation of the Lewis acid center to the non-bonding orbital of the Lewis basic center. The distance between the two Lewis centers of this species was found to be 3.073 Å, which is optimal for enabling H-H activation [20]. For comparison, its closed form (**I4′**-closed), with a strong B-N interaction ($R_{B\text{-}N}$ = 1.761 Å), was optimized (Fig. 4b), and found that this species is 10.3 kcal/mol higher in energy than its open form. Our computational attempts to enable H-H activation by species **I4′**-open form disclosed that there are two thermodynamically less favorable steps involved in this process (Fig. 5, red line): (i) formation of the σ-complex **I15**, and (ii) formation of zwitterion **I16** through splitting of H_2, with an overall TS barrier of 27.7 kcal/mol. Thus, foreseeing intermediate **I4′** as an FLP to split H_2 is less promising. Alternatively, in the second pathway (pathway b), the diindolyl borane intermediate **I18** lies relatively in a favored position at the free energy scale (2.8 kcal/mol), which is only slightly endergonic (ΔG = 4.3 kcal/mol) from the 3-BH_2 indoline intermediate (**I4**). The hydroboration energy barrier for this step to establish species **I18** is also achievable ($\Delta G^{\ddagger}$ = 22.0 kcal/mol) under RT or 60 °C. The optimized structure of species **I18** and its selected structural parameters are shown in Fig. 4c. As shown in this structure, this species displays the required orthogonal geometry around the Lewis centers to act as an intramolecular FLP for H_2 splitting. Like that of the 3-BH_2 indoline species **I4′**, the H_2 splitting process using species **I18** is endergonic (ΔG = 21.9 kcal/mol) with respect to the 3-BH_2 indoline intermediate (**I4**) with a barrier of 25.2 kcal/mol. Yet, in comparison of this step to that of **I4'** (pathway a) the H_2 splitting route enabled by species **I18** should be highly considered, especially at 60 °C. Therefore, for the consumption of H_2 in the reaction we postulate the heterolytic splitting of H_2 by **I18**, leading to a zwitterion **I19**, which might undergo the self-bimolecular protodeborylation reaction as shown in pathway b of Scheme 7.

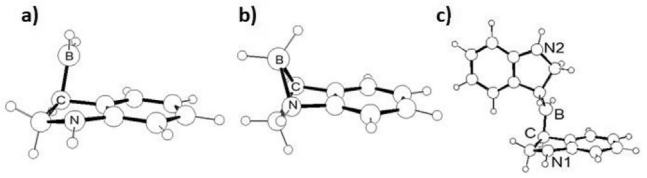

Fig. 4. DFT optimized structures of: (a) **I4′**-open, (b) **I4′**-closed, and (c) double hydroborated borane **I18**. Selected distances (Å) and angles (°) for: **I4′**-open, B-N = 3.073, B-C-N = 100.96; **I4′**-closed, B-N = 1.761, B-C-N = 53.89; **I18**, B-N1 = 3.186, B-C-N1 = 105.66.

2.8. Pathways for the formation of 1-Bpin indoline (*2a*) from 1-BH_2 indoline (*4a*)

As mentioned above in Scheme 4, the stoichiometric reaction

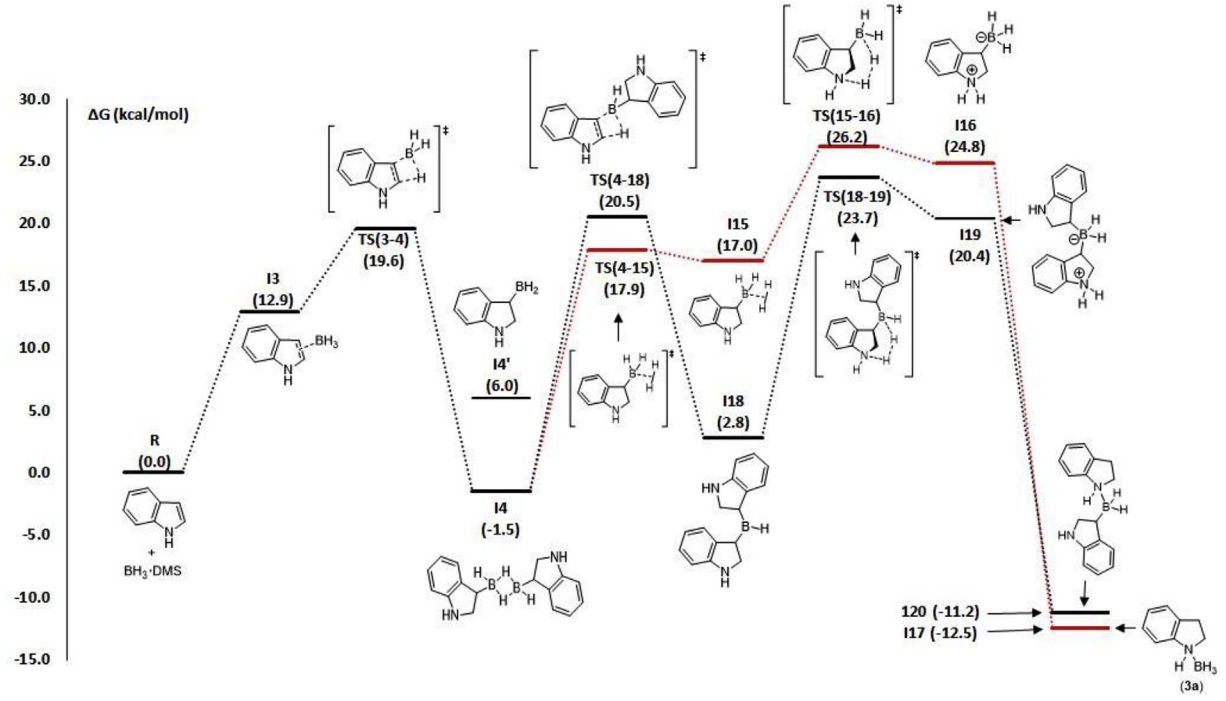

Fig. 5. Computed mechanistic pathways for the consumption of generated H_2 by the intermediates of hydroboration of indoles by BMS.

among indole, BMS and HBpin proceeds through intermediates 1-BH_2 indoline (**4a**) and diaminoborane (**5a**) to afford the product 1-Bpin indoline (**2a**). Noteworthy of this stoichiometric reaction is that the intermediate **4a** was only partially consumed while the intermediate **5a** is completely consumed for the formation of product **2a**. To understand the formation of **2a** from species **4a** and HBpin, computations were performed. The DFT results suppose that species 1-BH_2-indoline (**4a**′) is in equilibrium with dimer **4a** that has two dative N-B interactions, forming a four-membered B-N-B-N cycle. The dimeric species **4a** was found to be exergonic by 1.3 kcal/mol, and a barrier of 9.4 kcal/mol is required for the dissociation of **4a** to occur. From **4a**′ two pathways are possible to form 1-Bpin-indoline (**2a**). First, metathesis can occur directly between HBpin and **4a'** (Scheme 8, pathway a). Second, species **4a**′ can first disproportionate to observed diaminoborane species **5a**, which will then react with HBpin (Scheme 8, pathway b). Computationally, for the whole first pathway (pathway a) a high barrier was found for the initial metathesis step ($\Delta G^{\ddagger} = 17.2$ kcal/mol) (Fig. 6, red line). This energy barrier is easily attainable at RT or 60 °C. Albeit, the reason for the observation of some unreacted species **4a** and HBpin in the stoichiometric reaction is due to the fact that species **4a** and HBpin may exist in equilibrium with 1-Bpin indoline and BMS. This can be inferred from the computed pathway where the starting stage **I21** and the product stage **I28** were found to be nearly equal in energy. For the second pathway (pathway b), computations show that disproportionation is much facile (Fig. 6, black line). The high barrier in this pathway was found for the metathesis step between diaminoborane (**5a**) and HBpin. Between these two pathways for the transformation of species 1-BH_2 indoline (**4a**) to 1-Bpin indoline (**2a**), pathway b which involves disproportionation followed by metathesis is highly favored.

Overall, based on the experimental and computational insights, the plausible catalytic cycles for the formation of 1-Bpin indolines from indoles, HBpin and the catalyst BMS are presented in Fig. 7.

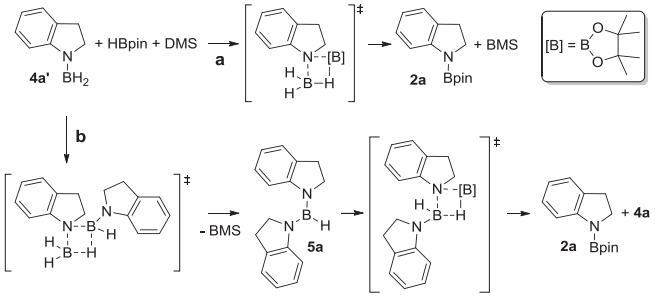

Scheme 8. Pathways perceived for the transformation of 1-BH_2 indoline to 1-Bpin indoline. Pathway a involves a direct metathesis step, and pathway b entails disproportionation and metathesis steps.

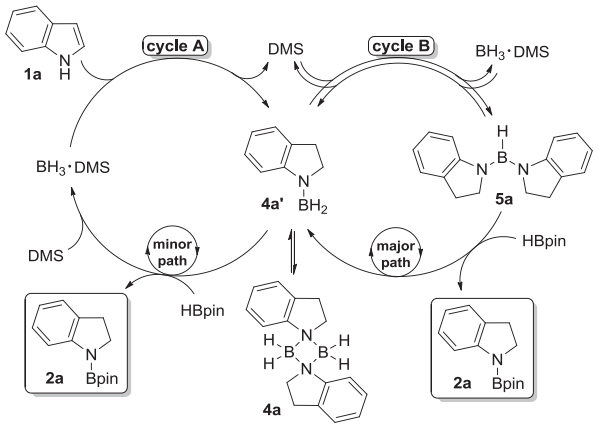

Fig. 7. Plausible catalytic cycles for the transformation of 1-BH_2 indoline to 1-Bpin indoline.

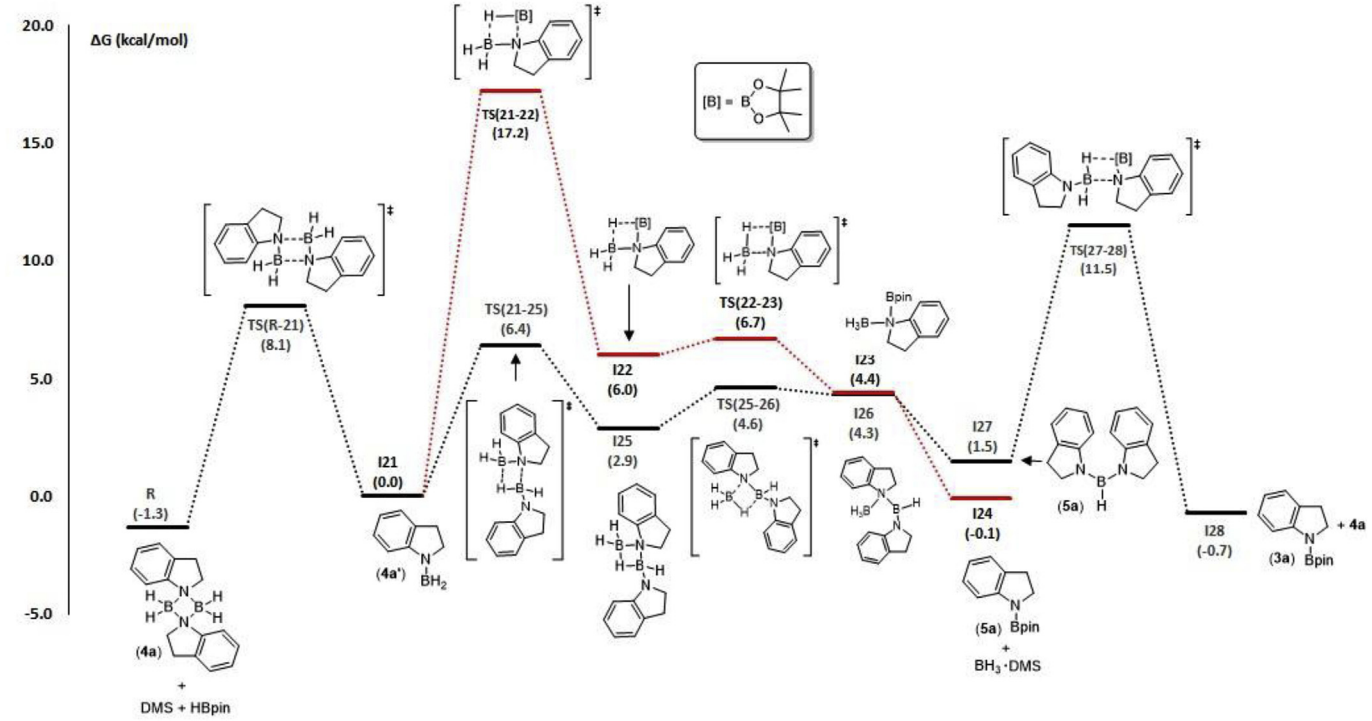

Fig. 6. Mechanistic pathways for conversion of 1-BH_2 indoline (**4a**) to 1-Bpin indoline (**2a**) using HBpin and its disproportionation to diaminoborane **5a** and BMS. [B] = Bpin.

Between the two catalytic cycles proposed, cycle B is more favored.

3. Conclusions

According to our experiments on the reaction of indoles with simple hydroboranes of the form $BH_3 \cdot$base, in either stoichiometric or catalytic quantity, the major resting state arose was 1-boryl indoline in an atom economical manner. In addition, only a minor proportion of H_2 was generated through a relatively less competitive side reaction. These insights overturn the earlier mechanistic proposal of generation of stoichiometric amount of H_2 along with the formation of the resting state intermediate 1-boryl indole. Through DFT computations we recognized that indoles likely undergo concerted hydroboration with simple hydroboranes, in a similar fashion to that of the alkenes, alkynes, enamines and enol ethers as previously reported. This step was ensued by double self protodeborylation of the formed hydroborated intermediates, 3-BH_2 indolines, to furnish the experimentally observed resting species 1-BH_2 indolines. A minor proportion of H_2 generated through a competing side reaction was observed to be consumed in the reaction. For its consumption, computations suggest the FLP-type heterolytic splitting of H_2 by a dihydroborated borane intermediate. Other computational mechanistic possibilities pursued based on the recent experimental observations from the reaction of unprotected and protected indoles with tertiary boranes can be ruled out for the formation of 1-BH_2 indolines from indoles and simple hydroboranes.

4. Experimental section

4.1. General comments

All procedures were carried out in a glovebox under a nitrogen atmosphere. All unprotected indoles were used as received from commercial suppliers. Dichloromethane, chloroform and $CDCl_3$ were purified by vacuum-distillation from P_2O_5. C_6D_6 was purified by vacuum distillation from Na/benzophenone. Pinacolborane (HBpin) was freshly prepared from BMS and pinacol in dichloromethane by following a literature procedure [21]. The prepared HBpin contains residual dichloromethane. The NMR spectra were recorded either on Agilent Technologies NMR spectrometer at 500.00 MHz (^{1}H), 125.757 MHz (^{13}C), 160.46 MHz (^{11}B) and 470.385 MHz (^{19}F) or on Varian Inova NMR AS400 spectrometer, at 400.0 MHz (^{1}H), 100.580 MHz (^{13}C) and 376.29 (^{19}F) in $CDCl_3$ or C_6D_6. Mass Spectrometry analyses were carried out on an Agilent 6210 LC Time of Flight Mass Spectrometer, by means of electrospray ionization (ESI) method.

4.2. Catalytic reactions

All catalytic reactions for the formation of 1-Bpin indolines were carried out using either J. Young NMR tubes or sealable 20 mL microwave vials. Indoles in a 0.1–0.5 mmol scale was first dissolved in chloroform or $CDCl_3$ (0.5–2 mL), then HBpin (1.0–1.3 equiv) and catalytic quantity of BMS (5 mol%) were introduced. This was followed by the tube was quickly sealed. The reaction mixture was subsequently heated at 60 °C for 2–3 h. Afterwards, solvent and other volatiles were evaporated in vacuo at RT for 2 h. Our attempts to crystallize the obtained products as residue in the form of either oil or powder led to decomposition under inert atmosphere and hydrolyzes if kept outside in a sealed flask. As a result, isolated yields were not possible and the obtained products as residue were characterized as soon as they were prepared. For characterization, the residue was dissolved in $CDCl_3$ for NMR spectroscopy. For mass spectrometry, a fraction (20 μL) of the $CDCl_3$ solution was taken and diluted with dichloromethane (1 mL).

4.2.1. 1-(4,4,5,5-Tetramethyl-1,3,2-dioxaborolan-2-yl)indoline (**2a**)

Reaction time: 3 h. Conversion: > 99%. ^{1}H NMR (500 MHz, $CDCl_3$): δ 7.29–7.27 (m, 1H), 7.13–7.06 (m, 2H), 6.77 (td, J = 7.4, 1.1 Hz, 1H), 3.78 (t, J = 8.8 Hz, 2H), 3.06 (t, J = 8.8 Hz, 2H), 1.31 (s, 12H). ^{13}C NMR (126 MHz, $CDCl_3$): δ 148.3, 131.4, 127.2, 124.4, 119.5, 112.6, 83.1, 47.0, 29.4, 24.7. ^{11}B NMR (160 MHz, $CDCl_3$): δ 23.8. HRMS (ESI-TOF) *m/z*: Calcd for $C_{14}H_{20}BNO_2 + H^+$: 245.1696; Found: 245.1646.

4.2.2. 5-Methoxy-1-(4,4,5,5-tetramethyl-1,3,2-dioxaborolan-2-yl) indoline (**2b**)

Reaction time: 3 h. Conversion: > 99%. ^{1}H NMR (500 MHz, $CDCl_3$): δ 7.15 (d, J = 8.6 Hz, 1H), 6.72 (d, J = 2.6 Hz, 1H), 6.63 (dd, J = 8.6, 2.7 Hz, 1H), 3.78 (t, J = 8.7 Hz, 2H), 3.75 (s, 3H), 3.02 (t, J = 8.7 Hz, 2H), 1.29 (s, 12H). ^{13}C NMR (126 MHz, $CDCl_3$): δ 153.7, 142.1, 132.7, 112.6, 112.2, 111.0, 83.1, 55.9, 47.3, 29.9, 24.7. ^{11}B NMR (160 MHz, $CDCl_3$): δ 23.5. HRMS (ESI-TOF) *m/z*: Calcd for $C_{15}H_{22}BNO_3 + H^+$: 276.1766; Found: 276.1750.

4.2.3. 6-Methyl-1-(4,4,5,5-tetramethyl-1,3,2-dioxaborolan-2-yl) indoline (**2c**)

Reaction time: 3 h. Conversion: 98%. ^{1}H NMR (500 MHz, $CDCl_3$): δ 7.09 (s, 1H), 6.98 (d, J = 7.5 Hz, 1H), 6.60–6.57 (m, 1H), 3.76 (t, J = 8.8 Hz, 2H), 3.00 (t, J = 8.7 Hz, 2H), 2.31 (s, 3H), 1.31 (s, 12H). ^{13}C NMR (126 MHz, $CDCl_3$): δ 148.4, 137.0, 128.5, 124.0, 120.3, 113.3, 83.1, 47.3, 29.1, 24.7, 21.7. ^{11}B NMR (160 MHz, $CDCl_3$): δ 23.5. HRMS (ESI-TOF) *m/z*: Calcd for $C_{15}H_{22}BNO_2 + H^+$: 260.1819; Found: 260.1811.

4.2.4. 5-Fluoro-1-(4,4,5,5-tetramethyl-1,3,2-dioxaborolan-2-yl) indoline (**2d**)

Reaction time: 3 h. Conversion: 97%. ^{1}H NMR (500 MHz, $CDCl_3$): δ 7.15 (dd, J = 8.6, 4.7 Hz, 1H), 6.83–6.79 (m, 1H), 6.78–6.72 (m, 1H), 3.78 (t, J = 9.0 Hz, 2H), 3.03 (t, J = 9.2 Hz, 2H), 1.30 (s, 12H). ^{13}C NMR (126 MHz, $CDCl_3$): δ 157.3 (d, J = 236.1 Hz), 144.3, 125.9, 113.1 (d, J = 22.9 Hz), 112.6 (d, J = 8.1 Hz), 111.6 (d, J = 23.8 Hz), 83.1, 47.4, 29.6, 24.7. ^{11}B NMR (160 MHz, $CDCl_3$): δ 23.5. HRMS (ESI-TOF) *m/z*: Calcd for $C_{14}H_{19}BFNO_2 + H^+$: 264.1568; Found: 264.1565.

4.2.5. 5-Chloro-1-(4,4,5,5-tetramethyl-1,3,2-dioxaborolan-2-yl) indoline (**2e**)

Reaction time: 3 h. Conversion: > 99%. ^{1}H NMR (500 MHz, $CDCl_3$): δ 7.14 (dd, J = 8.4, 0.4 Hz, 1H), 7.05–6.95 (m, 2H), 3.75 (t, J = 9.2 Hz, 2H), 3.01 (t, J = 8.8 Hz, 2H), 1.28 (s, 12H). ^{11}B NMR (160 MHz, $CDCl_3$): δ 23.7. HRMS (ESI-TOF) *m/z*: Calcd for $C_{14}H_{19}BClNO_2 + H^+$: 280.1273; Found: 280.1259.

4.2.6. 5-Bromo-1-(4,4,5,5-tetramethyl-1,3,2-dioxaborolan-2-yl) indoline (**2f**)

Reaction time: 3 h. Conversion: 96%.^{1}H NMR (500 MHz, $CDCl_3$): δ 7.18–7.13 (m, 1H), 7.12–7.08 (m, 2H), 3.74 (t, J = 9.0 Hz, 2H), 3.01 (t, J = 8.8 Hz, 2H), 1.28 (s, 12H). ^{11}B NMR (160 MHz, $CDCl_3$): δ 23.6. HRMS (ESI-TOF) *m/z*: Calcd for $C_{14}H_{19}BBrNO_2 + H^+$: 324.0768; Found: 324.0753.

4.2.7. 6-Fluoro-1-(4,4,5,5-tetramethyl-1,3,2-dioxaborolan-2-yl) indoline (**2g**)

Reaction time: 3 h. Conversion: > 99%. ^{1}H NMR (500 MHz, $CDCl_3$): δ 7.03–6.91 (m, 2H), 6.41 (ddd, J = 9.3, 8.1, 2.4 Hz, 1H), 3.78 (d, J = 9.1 Hz, 2H), 2.98 (t, J = 8.8 Hz, 2H), 1.29 (s, 12H). ^{11}B NMR (160 MHz, $CDCl_3$): δ 23.8. ^{19}F NMR (470 MHz, $CDCl_3$): δ −114.9. HRMS (ESI-TOF) *m/z*: Calcd for $C_{14}H_{19}BFNO_2 + H^+$: 264.1568; Found: 264.1561.

4.2.8. 6-Chloro-1-(4,4,5,5-tetramethyl-1,3,2-dioxaborolan-2-yl) indoline (**2h**)

Reaction time: 3 h. Conversion: 98%. ^{1}H NMR (500 MHz, $CDCl_3$): δ 7.21 (s, 1H), 6.96 (d, J = 7.0 Hz, 1H), 6.69 (d, J = 7.8 Hz, 1H), 3.77 (t, J = 8.8 Hz, 2H), 2.99 (t, J = 8.8 Hz, 2H), 1.29 (s, 12H). ^{11}B NMR (160 MHz, $CDCl_3$): δ 23.6. HRMS (ESI-TOF) *m/z*: Calcd for $C_{14}H_{19}BClNO_2 + H^+$: 280.1273; Found: 280.1257.

4.2.9. 6-Bromo-1-(4,4,5,5-tetramethyl-1,3,2-dioxaborolan-2-yl) indoline (**2i**)

Reaction time: 3 h. Conversion: > 99%. ^{1}H NMR (500 MHz, $CDCl_3$): δ 7.36 (d, J = 1.8 Hz, 1H), 6.92 (d, J = 7.8 Hz, 1H), 6.85 (dd, J = 7.8, 1.8 Hz, 1H), 3.76 (t, J = 8.8 Hz, 2H), 2.97 (t, J = 8.8 Hz, 2H), 1.29 (s, 12H). ^{11}B NMR (160 MHz, $CDCl_3$): δ 23.6. HRMS (ESI-TOF) *m/z*: Calcd for $C_{14}H_{19}BBrNO_2 + H^+$: 324.0768; Found: 324.0752.

4.2.10. 4-Chloro-1-(4,4,5,5-tetramethyl-1,3,2-dioxaborolan-2-yl) indoline (**2j**)

Reaction time: 3 h. Conversion: 97%. ^{1}H NMR (500 MHz, $CDCl_3$): δ 7.14 (dd, J = 8.0, 0.9 Hz, 1H), 7.00 (tt, J = 8.0, 0.8 Hz, 1H), 6.73 (dd, J = 8.0, 0.9 Hz, 1H), 3.80 (t, J = 9.2 Hz, 2H), 3.09 (t, J = 8.9 Hz, 2H), 1.30 (s, 12H). ^{13}C NMR (126 MHz, $CDCl_3$): δ 149.8, 130.4, 129.8, 128.7, 119.4, 110.7, 83.1, 46.7, 28.9, 24.7. ^{11}B NMR (160 MHz, $CDCl_3$): δ 23.2. HRMS (ESI-TOF) *m/z*: Calcd for HRMS (ESI-TOF) *m/z*: Calcd for $C_{14}H_{19}BClNO_2 + H^+$: 280.1273; Found: 280.1251.

4.2.11. 5-Nitro-1-(4,4,5,5-tetramethyl-1,3,2-dioxaborolan-2-yl) indoline (**2k**)

Reaction time: 4 h. Conversion: > 99%. ^{1}H NMR (500 MHz, $CDCl_3$): δ 7.99 (d, J = 8.9 Hz, 1H), 7.93 (s, 1H), 7.24 (d, J = 9.2 Hz, 1H), 3.86 (t, J = 8.9 Hz, 2H), 3.10 (t, J = 8.9 Hz, 2H), 1.30 (s, 12H). ^{11}B NMR (160 MHz, $CDCl_3$): δ 23.9. HRMS (ESI-TOF) *m/z*: Calcd for $C_{14}H_{19}BN_2O_4 + H^+$: 290.1438; Found: 290.1433.

4.2.12. 6-Nitro-1-(4,4,5,5-tetramethyl-1,3,2-dioxaborolan-2-yl) indoline (**2l**)

Reaction time: 6 h. Conversion: 98%. ^{1}H NMR (500 MHz, $CDCl_3$): δ 7.97 (d, J = 2.2 Hz, 1H), 7.63 (dd, J = 8.1, 2.2 Hz, 1H), 7.14 (d, J = 8.1 Hz, 1H), 3.85 (t, J = 8.9 Hz, 2H), 3.11 (t, J = 8.6 Hz, 2H), 1.31 (s, 12H). ^{13}C NMR (126 MHz, $CDCl_3$): δ 149.7, 148.3, 139.2, 124.1, 115.5, 107.2, 83.1, 47.6, 29.2, 24.7. ^{11}B NMR (160 MHz, $CDCl_3$): δ 23.9. HRMS (ESI-TOF) *m/z*: Calcd for $C_{14}H_{19}BN_2O_4 + H^+$: 290.1438; Found: 290.1426.

4.2.13. 7-Fluoro-1-(4,4,5,5-tetramethyl-1,3,2-dioxaborolan-2-yl) indoline (**2m**)

Reaction time: 16 h. Conversion: 75%. ^{1}H NMR (500 MHz, $CDCl_3$): δ 6.90 (dq, J = 7.2, 1.1 Hz, 1H), 6.84 (dddt, J = 11.0, 8.2, 1.3, 0.8 Hz, 1H), 6.74 (ddd, J = 8.2, 7.2, 4.3 Hz, 1H), 3.83 (t, J = 8.4 Hz, 2H), 3.01 (t, J = 8.4 Hz, 2H), 1.31 (s, 1H). ^{13}C NMR (126 MHz, $CDCl_3$): δ 151.1, 149.1, 136.7, 136.7, 134.4, 134.3, 121.2, 121.1, 119.8, 119.8, 115.2, 115.0, 82.9, 49.7, 30.4, 24. 6. ^{11}B NMR (160 MHz, $CDCl_3$): δ 23.5. ^{19}F NMR (470 MHz): δ −124.6. HRMS (ESI-TOF) *m/z*: Calcd for $C_{14}H_{19}BFNO_2 + H^+$: 264.1568; Found: 264.1559.

4.2.14. 7-Methyl-1-(4,4,5,5-tetramethyl-1,3,2-dioxaborolan-2-yl) indoline (**2n**)

Reaction time: 16 h. Conversion: 43%. ^{1}H NMR (500 MHz, $CDCl_3$): δ 7.05–7.02 (m, 1H), 6.96–6.83 (m, 1H), 6.72 (m, 1H), 3.60 (t, J = 8.4 Hz, 2H), 3.10 (t, J = 8.4 Hz, 2H), 2.19 (s, 3H), 1.30 (s, 12H). ^{11}B NMR (160 MHz, $CDCl_3$): δ 21.2. HRMS (ESI-TOF) *m/z*: Calcd for $C_{15}H_{22}BNO_2 + H^+$: 260.1819; Found: 260.1813.

4.3. Stoichiometric and sub-stoichiometric reactions

All stoichiometric and sub-stoichiometric reactions were carried out using J. Young NMR tubes in $CDCl_3$ at various temperatures and reaction hours. For monitoring the reaction between indole and BMS, indole (**1a**, 0.1 mmol, 11.7 mg) and BMS (0.1 mmol, 9.5 μL) dissolved in 0.5 mL $CDCl_3$ was employed at different temperatures. To understand the equilibrium between 1-BH_2 indoline (**4a**) and diaminoborane (**5a**) from the disproportionation reaction, the ratio between indole and BMS was varied by keeping indole at 0.1 mmol and varying BMS quantity from 0.2 to 0.05 mmol.

4.4. Computational details

Geometry optimizations and frequency calculations were performed at the hybrid DFT with dispersion-corrected functional ωB97XD [22], as implemented in the Gaussian 09 (revision C.01) software program [23]. The standard 6-31G(d,p) basis set was used. Transition state (TS) geometries were obtained using opt = (ts, noeigentest, calcfc) algorithms [24]. Frequency calculations were performed on all optimized structures to verify the nature of the structures and to extract the thermochemistry information. From the frequency calculations we ensured that the TS structures had only one imaginary frequency and that the magnitudes of all frequencies were greater than the residual frequencies that are due to rotations and translations. Additionally, each TS was confirmed to be on the chosen reaction path by performing "plus-and-minus-displacement" minimization calculations where the TS structure was displaced ca. 0.05 Å or 5° on the imaginary frequency normal mode in both directions and subsequently the displaced geometries were optimized to the nearest minima [25]. The energies (ΔG) given are corrected for zero-point vibrational energies.

Acknowledgments

We gratefully acknowledge National Sciences and Engineering Research Council of Canada (NSERC) and Centre de Catalyse et Chimie Verte (Quebec) for funding, and Compute Canada (Calcul-Quebec and Graham) for computational resources. F.-G.F. also thanks NSERC for the award of a Canada Research Chair.

Appendix A. Supplementary data

Supplementary data to this article can be found online at https://doi.org/10.1016/j.tet.2019.02.048.

References

[1] (a) R.H. Fish, J.L. Tan, A.D. Thormodsen, Organometallics 4 (1985) 1743–1747;
(b) M. Rosales, J. Navarro, L. Sánchez, A. González, Y. Alvarado, R. Rubio, C. De La Cruz, T. Rajmankina, Trans. Met. Chem. 21 (1996) 11–15;
(c) R. Kuwano, K. Sato, T. Kurokawa, D. Karube, Y. Ito, J. Am. Chem. Soc. 122 (2000) 7614–7615;
(d) C. Bianchini, A. Meli, F. Vizza, Eur. J. Inorg. Chem. 2001 (2000) 43–68;
(e) P. Barbaro, C. Bianchini, A. Meli, M. Moreno, F. Vizza, Organometallics 21 (2002) 1430–1437.
[2] (a) G.W. Gribble, P.D. Lord, J. Skotnicki, S.E. Dietz, J.T. Eaton, J. Johnson, J. Am. Chem. Soc. 96 (1974) 7812–7814;
(b) W. Gribble, G., Chem. Soc. Rev. 27 (1998) 395–404;
(c) B.E. Maryanoff, D.F. McComsey, J. Org. Chem. 43 (1978) 2733–2735;
(d) K.M. Biswas, R. Dhara, S. Roy, H. Mallik, Tetrahedron 40 (1984) 4351–4357;
(e) J.G. Berger, Synthesis 1974 (1974) 508–510;
(f) J. Seyden-Penne, Reductions by the Alumino- and Borohydride in Organic Synthesis, 2 ed., Wiley-VCH, New York, 1997;
(g) S.A. Monti, R.R. Schmidt III, Tetrahedron 27 (1971) 3331–3339.
[3] M. Bandini, Org. Biomol. Chem. 11 (2013) 5206–5212.
[4] G.B. Fisher, C.T. Goralski, L.W. Nicholson, D.L. Hasha, D. Zakett, B. Singaram, J. Org. Chem. 60 (1995) 2026–2034.
[5] (a) M.A. Légaré, M.A. Courtemanche, E. Rochette, F.G. Fontaine, Science 349

(2015) 513–516;
(b) J. Légaré-Lavergne, A. Jayaraman, L.C. Misal Castro, É. Rochette, F.-G. Fontaine, J. Am. Chem. Soc. 139 (2017) 14714–14723;
(c) A. Jayaraman, L.C. Misal Castro, F.-G. Fontaine, Org. Process Res. Dev. 22 (2018) 1489–1499.
[6] (a) F. Focante, I. Camurati, D. Nanni, R. Leardini, L. Resconi, Organometallics 23 (2004) 5135–5141;
(b) M.A. Dureen, C.C. Brown, D.W. Stephan, Organometallics 29 (2010) 6422–6432.
[7] (a) A. Jayaraman, L.C. Misal Castro, V. Desrosiers, F.-G. Fontaine, Chem. Sci. 9 (2018) 5057–5063;
(b) N.W.J. Ang, C.S. Buettner, S. Docherty, A. Bismuto, J.R. Carney, J.H. Docherty, M.J. Cowley, S.P. Thomas, Synthesis 50 (2018) 803–808.
[8] In contrast, the stoichiometric reaction between these substrates and BMS led to a complete consumption of the substrate and formation of multiple unidentifiable species.
[9] The same also works without addition of catalytic amount of BMS, but requires an elevated temperature (80 °C) and a long reaction time (16 h).
[10] The same products can also be obtained at room temperature but requires a long reaction time (~48 h).
[11] E.A. Romero, J.L. Peltier, R. Jazzar, G. Bertrand, Chem. Commun. 52 (2016) 10563–10565.
[12] X. Chen, J.-C. Zhao, S.G. Shore, J. Am. Chem. Soc. 132 (2010) 10658–10659.
[13] W. Friedrichsen, T. Traulsen, J. Elguero, A.R. Katritzky, Tautomerism of heterocycles: five-membered rings with one heteroatom, in: A.R. Katritzky (Ed.), Advances in Heterocyclic Chemistry, vol. 76, Academic Press, 2000, pp. 85–156.
[14] M. Nakagawa, T. Hino, Tetrahedron 26 (1970) 4491–4503.
[15] I.G. Gut, J. Wirz, Angew. Chem. Int. Ed. 33 (1994) 1153–1156.
[16] S. Guidotti, I. Camurati, F. Focante, L. Angellini, G. Moscardi, L. Resconi, R. Leardini, D. Nanni, P. Mercandelli, A. Sironi, T. Beringhelli, D. Maggioni, J. Org. Chem. 68 (2003) 5445–5465.
[17] (a) F.-G. Fontaine, D.W. Stephan, Phil. Trans. R. Soc. A (2017) 375;
(b) D.W. Stephan, Science 354 (2016) 6317;
(c) F.-G. Fontaine, É. Rochette, Acc. Chem. Res. 51 (2018) 454–464;
(d) D.W. Stephan, G. Erker, Angew. Chem. Int. Ed. 54 (2015) 6400–6441;
(e) D.W. Stephan, J. Am. Chem. Soc. 137 (2015) 10018–10032;
(f) D.W. Stephan, Acc. Chem. Res. 48 (2015) 306–316;
(g) G. Erker, D.W. Stephan, Frustrated Lewis Pairs I and II, Springer, New York, 2013.
[18] (a) D.W. Stephan, G. Erker, Angew. Chem. Int. Ed. 49 (2009) 46–76;
(b) T.A. Rokob, A. Hamza, A. Stirling, T. Soós, I. Pápai, Angew. Chem. Int. Ed. 47 (2008) 2435–2438;
(c) P.A. Chase, D.W. Stephan, Angew. Chem. Int. Ed. 47 (2008) 7433–7437;
(d) K. Chernichenko, M. Nieger, M. Leskelä, T. Repo, Dalton Trans. 41 (2012) 9029–9032;
(e) K. Chernichenko, B. Kótai, I. Pápai, V. Zhivonitko, M. Nieger, M. Leskelä, T. Repo, Angew. Chem. Int. Ed. 54 (2014) 1749–1753;
(f) M.-A. Courtemanche, É. Rochette, M.-A. Légaré, W. Bi, F.-G. Fontaine, Dalton Trans. 45 (2016) 6129–6135.
[19] (a) H.C. Brown, G.J. Klender, Inorg. Chem. 1 (1962) 204–214;
(b) Jayaraman, A.; Desrosiers, V., Unpublished Results. Université Laval: 2017.
[20] (a) V. Sumerin, K. Chernichenko, F. Schulz, M. Leskelä, B. Rieger, T. Repo, Amine-borane mediated metal-free hydrogen activation and catalytic hydrogenation, in: G. Erker, D.W. Stephan (Eds.), Frustrated Lewis Pairs I: Uncovering and Understanding, Springer Berlin Heidelberg, Berlin, Heidelberg, 2013, pp. 111–155;
(b) F. Schulz, V. Sumerin, S. Heikkinen, B. Pedersen, C. Wang, M. Atsumi, M. Leskelä, T. Repo, P. Pyykkö, W. Petry, B. Rieger, J. Am. Chem. Soc. 133 (2011) 20245–20257.
[21] A. Macé, S. Touchet, P. Andres, F. Cossío, V. Dorcet, F. Carreaux, B. Carboni, Angew. Chem. Int. Ed. 55 (2016) 1025–1029.
[22] J.-D. Chai, M. Head-Gordon, Phys. Chem. Chem. Phys. 10 (2008) 6615–6620.
[23] M.J.T. Frisch, G. W, H.B. Schlegel, G.E. Scuseria, M.A. Robb, J.R. Cheeseman, G. Scalmani, V. Barone, G.A. Petersson, H. Nakatsuji, X. Li, M. Caricato, A. Marenich, J. Bloino, B.G. Janesko, R. Gomperts, B. Mennucci, H.P. Hratchian, J.V. Ortiz, A.F. Izmaylov, J.L. Sonnenberg, D. Williams-Young, F. Ding, F. Lipparini, F. Egidi, J. Goings, B. Peng, A. Petrone, T. Henderson, D. Ranasinghe, V.G. Zakrzewski, J. Gao, N. Rega, G. Zheng, W. Liang, M. Hada, M. Ehara, K. Toyota, R. Fukuda, J. Hasegawa, M. Ishida, T. Nakajima, Y. Honda, O. Kitao, H. Nakai, T. Vreven, K. Throssell, Montgomery Jr., J.A., J.E. Peralta, F. Ogliaro, M. Bearpark, J.J. Heyd, E. Brothers, K.N. Kudin, V.N. Staroverov, T. Keith, R. Kobayashi, J. Normand, K. Raghavachari, A. Rendell, J.C. Burant, S.S. Iyengar, J. Tomasi, M. Cossi, J.M. Millam, M. Klene, C. Adamo, R. Cammi, J.W. Ochterski, R.L. Martin, K. Morokuma, O. Farkas, J.B. Foresman, D.J. Fox, Gaussian, Gaussian Inc., Wallingford CT, 2016.
[24] (a) J. Baker, J. Comput. Chem. 7 (1986) 385–395;
(b) C. Peng, P.Y. Ayala, H.B. Schlegel, M.J. Frisch, J. Comput. Chem. 17 (1996) 49–56.
[25] (a) A. Jayaraman, A.L.L. East, J. Org. Chem. 77 (2012) 351–356;
(b) A. Jayaraman, G.M. Berner, L.M. Mihichuk, A.L.L. East, J. Mol. Catal. Chem. 351 (2011) 143–153;
(c) A.L.L. East, G.M. Berner, A.D. Morcom, L. Mihichuk, J. Chem. Theor. Comput. 4 (2008) 1274–1282.